

LETTER • OPEN ACCESS

High potential for loss of permafrost landforms in a changing climate

Recent citations

- [Rock glaciers and related cold rocky landforms: Overlooked climate refugia for mountain biodiversity](#)
Stefano Brighenti *et al*

To cite this article: Olli Karjalainen *et al* 2020 *Environ. Res. Lett.* **15** 104065

View the [article online](#) for updates and enhancements.

Environmental Research Letters



LETTER

High potential for loss of permafrost landforms in a changing climate

OPEN ACCESS

RECEIVED
20 April 2020

REVISED
12 August 2020

ACCEPTED FOR PUBLICATION
17 August 2020

PUBLISHED
2 October 2020

Original content from this work may be used under the terms of the [Creative Commons Attribution 4.0 licence](#).

Any further distribution of this work must maintain attribution to the author(s) and the title of the work, journal citation and DOI.



Olli Karjalainen¹ , Miska Luoto² , Juha Aalto^{2,3} , Bernd Etzelmüller⁴ , Guido Grosse^{5,6} , Benjamin M Jones⁷ , Karianne S Lilleøren⁴ and Jan Hjort¹

¹ Geography Research Unit, University of Oulu, P.O. Box 3000, Oulu 90014, Finland

² Department of Geosciences and Geography, University of Helsinki, P.O. Box 64, Helsinki 00014, Finland

³ Finnish Meteorological Institute, P.O. Box 503, Helsinki 00101, Finland

⁴ Department of Geosciences, University of Oslo, P.O. Box 1047, Oslo 0316, Norway

⁵ Alfred Wegener Institute, Helmholtz Centre for Polar and Marine Research, Potsdam 14773, Germany

⁶ University of Potsdam, Institute of Geosciences, Potsdam 14776, Germany

⁷ Institute of Northern Engineering, University of Alaska Fairbanks, P.O. Box 755860, Alaska, 99775, Fairbanks, United States of America

E-mail: olli.karjalainen@oulu.fi

Keywords: permafrost, climate change, ground ice, environmental change, environmental space, geodiversity, statistical ensemble modelling

Supplementary material for this article is available [online](#)

Abstract

The presence of ground ice in Arctic soils exerts a major effect on permafrost hydrology and ecology, and factors prominently into geomorphic landform development. As most ground ice has accumulated in near-surface permafrost, it is sensitive to variations in atmospheric conditions. Typical and regionally widespread permafrost landforms such as pingos, ice-wedge polygons, and rock glaciers are closely tied to ground ice. However, under ongoing climate change, suitable environmental spaces for preserving landforms associated with ice-rich permafrost may be rapidly disappearing. We deploy a statistical ensemble approach to model, for the first time, the current and potential future environmental conditions of three typical permafrost landforms, pingos, ice-wedge polygons and rock glaciers across the Northern Hemisphere. We show that by midcentury, the landforms are projected to lose more than one-fifth of their suitable environments under a moderate climate scenario (RCP4.5) and on average around one-third under a very high baseline emission scenario (RCP8.5), even when projected new suitable areas for occurrence are considered. By 2061–2080, on average more than 50% of the recent suitable conditions can be lost (RCP8.5). In the case of pingos and ice-wedge polygons, geographical changes are mainly attributed to alterations in thawing-season precipitation and air temperatures. Rock glaciers show air temperature-induced regional changes in suitable conditions strongly constrained by topography and soil properties. The predicted losses could have important implications for Arctic hydrology, geo- and biodiversity, and to the global climate system through changes in biogeochemical cycles governed by the geomorphology of permafrost landscapes. Moreover, our projections provide insights into the circumpolar distribution of various ground ice types and help inventory permafrost landforms in unmapped regions.

1. Introduction

The presence of ground ice in the surface layers of permafrost is central to the geomorphic and hydro-ecological functioning of high-latitude and altitude permafrost landscapes (Rowland *et al* 2010, Kokelj *et al* 2014, Liljedahl *et al* 2016). Involved geomorphic processes give rise to permafrost landforms, such as

ice-cored pingo mounds (Mackay 1988), ice wedges that form distinctive polygonal patterned ground (Washburn 1980), and slowly creeping rock glaciers in mountains (Barsch 1996). Ice-rich permafrost landforms are responsive to climatic perturbations as indicated by the intensified permafrost degradation during the past decades (Liljedahl *et al* 2016, Farquharson *et al* 2019). Relict permafrost landforms

found in temperate climates (e.g. pingo remnants and ice-wedge casts in western and central Europe (Vandenberghe and Pissart 1993) imply that distributions of permafrost landforms have changed before and are likely to change in future climates (Washburn 1980, Grosse and Jones 2011, Liljedahl *et al* 2016).

Projected increases in air temperatures and precipitation with Arctic amplification (Hoegh-Guldberg *et al* 2018) are anticipated to intensify permafrost warming (Biskaborn *et al* 2019) and associated thermokarst processes, i.e. thawing and settling of ice-rich permafrost (Jorgenson *et al* 2006, Grosse *et al* 2016, Douglas *et al* 2020). Landscapes with current thermokarst features or susceptibility to future thermokarst are estimated to cover up to 20% of circumpolar permafrost regions (Olefeldt *et al* 2016). Rising air and ground temperatures pose a potential constraint for pingo persistence across northern Siberia (Grosse and Jones 2011), Alaska (Jones *et al* 2012), and Canada (Mackay 1988), for example. Degradation of ice-wedge polygons has been observed across the Arctic, including continuous permafrost regions (Jorgenson *et al* 2006, 2015, Grosse *et al* 2016, Liljedahl *et al* 2016, Steedman *et al* 2017, Fraser *et al* 2018, Farquharson *et al* 2019). Moreover, downslope creeping of rock glaciers due to ground ice deformation has shown increased surface velocities related to increased air temperatures in some regions (Kääb *et al* 2007, Jones *et al* 2019). The degradation of ground ice in permafrost landforms can induce thermokarst or mass-movement hazards (Kääb *et al* 2007) and thereby threaten infrastructure development (Rowland *et al* 2010, Kanevskiy *et al* 2017, Hjort *et al* 2018, Streletskiy *et al* 2019).

Permafrost landforms bear local-scale geomorphic (Humlum 2000, Knight *et al* 2019, Ward Jones *et al* 2019), hydrological (Liljedahl *et al* 2016, Brighenti *et al* 2019, Nitzbon *et al* 2019) and biological (Lara *et al* 2018) significance, but also affect global systems through alterations in atmospheric (Schuur *et al* 2015) and aquatic (Serikova *et al* 2018) greenhouse gas fluxes from permafrost regions. These landforms also contribute to local biodiversity (Jorgenson *et al* 2006) by serving as highly specialized ecosystems for flora (Jorgenson *et al* 2015) and fauna (Fountain *et al* 2012). In some regions they also provide a freshwater supply for human use (Jones *et al* 2018).

At present, the information on current and potential future distributions of permafrost landforms at the circumpolar scale is sparse. This is despite an increasing amount of circumpolar to global permafrost extent simulations conducted both with process-based (e.g. Guo and Wang 2016) and empirical/statistical approaches (Chadburn *et al* 2017, Aalto *et al* 2018, Obu *et al* 2019). The lack of spatially detailed knowledge on geomorphic features poses a limitation to the assessments of climate change impacts on permafrost environments. We aim to reduce these

knowledge gaps by applying statistical distribution modelling. Statistical modelling methods have been used in geomorphological contexts (Luoto *et al* 2010, Aalto *et al* 2014, Rudy *et al* 2017, Fewster *et al* 2020). In our previous work (Aalto *et al* 2018), we have demonstrated that a statistical approach produces similar permafrost extents with process-based models (e.g. Guo and Wang 2016) and other empirical models (Chadburn *et al* 2017, Obu *et al* 2019), and have relatively small prediction errors. The advantage of the approach over physically based models which require extensive parameterization of physical soil properties, for example, is that statistical modelling allows for predicting landform occurrence at high spatial resolution across the circumpolar region using readily available geospatial data on climate, soil and topography. Thus, our approach does not consider various processes affecting heat fluxes or ground ice accumulation in permafrost but is suitable for examining how different environmental factors affect the distribution of permafrost landforms across the circumpolar region.

Our objective is to model, for the first time, the potential environmental spaces for the occurrence of pingos, ice-wedge polygons and rock glaciers across the Northern Hemisphere. These spaces encompass conditions where climate, topography and soil properties are suitable for landform presence. In the modelling we assumed the landforms to be in equilibrium with climate conditions for the considered period, that is, we did not make assumptions concerning whether the landforms are degrading or still growing. Based on the statistical modelling results, we present the circumpolar coverages of potential environmental spaces for the studied landforms during a recent period (1950–2000) and predict their regional changes for two future periods (2041–2060 and 2061–2080) using representative concentration pathway RCP4.5 (stabilization scenario) and RCP8.5 (rising radiative forcing pathway) climate-change scenarios. Moreover, the results offer insights into the fine-scale distribution of various ground ice types and help inventory permafrost landforms in unmapped regions.

2. Materials and methods

2.1. Permafrost landform observations

Observations of pingos, ice-wedge polygons and rock glaciers across the Northern Hemisphere (i.e. presence data, figure 1(a)) made since late 20th century were compiled from available inventories, published studies and geomorphological maps (see section S1 (available online at stacks.iop.org/ERL/15/104065/mmedia) in supplementary material). Ice-cored pingo mounds (figure 1(b)) form in permafrost environments by injection and freezing of pressurized water in the soil, and results in massive-ice formation and upheaving

of overlying surface material (Mackay 1988). Two primary pingo types are often distinguished: hydrostatic, predominantly occurring in low-lying continuous permafrost regions, and hydraulic, which are more typical to discontinuous permafrost and depend on water moving under a hydraulic gradient (Mackay 1988, Grosse and Jones 2011, Jones *et al* 2012). Distinct patterned ground features, ice-wedge polygons (figure 1(c)), occur nearly ubiquitously in unconsolidated deposits across the Northern Hemisphere permafrost domain and wedge ice is the most common form of ground ice in continuous permafrost (Bernard-Grand'Maison and Pollard 2018). The polygon shape results from the cyclical growth of ice wedges in thermal contraction cracks formed in susceptible soils during cold spells in wintertime (Washburn 1980, Kokelj *et al* 2014).

Rock glaciers are bodies of poorly sorted debris and ice that move due to deformation of internal ice (Barsch 1996, Berthling 2011, figure 1(d)) in permafrost environments. They occupy most mountain regions in both continental and maritime climates including high-Arctic conditions (Evans 1993) and high elevations in warmer climates in, e.g. the Middle East (Gorbulov 2013). We included both active (flowing or creeping downward) and inactive (stagnant) rock glaciers that contain ice (Barsch 1996) regardless of whether they were primarily influenced by talus slope dynamics or by glacier dynamics (moraine-derived rock glaciers) (see section S1, supplementary material) but excluded relict landforms. In addition to presence data, the applied modelling required information on environments where the landforms are not present. Thus, we compiled datasets with 1349 absence grid cells for pingos, 494 for ice-wedge polygons and 1549 for rock glaciers (section S1, supplementary material).

2.2. Environmental data

In general, the formation of ground ice and associated landforms require permafrost conditions with efficient wintertime freezing and reasonably cool summers (Washburn 1980, Mackay 1988). Moreover, rainfall, topography, and properties of snow, vegetation and soil layers affect ground ice accumulation and preservation potential in the landforms (Barsch 1996, Boeckli *et al* 2012, Bernard-Grand'Maison and Pollard 2018, Knight *et al* 2019, Douglas *et al* 2020). We used geospatial data on physically relevant factors (climate, soil and topography predictors) at 30 arc-second (~1 km) spatial resolution to examine their effects on landform occurrence.

To account for the assumed seasonal effects of climate we computed freezing and thawing degree-days (FDD and TDD, °C-days) and amounts of solid (Snowfall, mm) and liquid (Rainfall, mm) precipitation. Snowfall was defined as the sum of precipitation

for months with average air temperature below 0 °C, and rainfall for those above 0 °C. The variables were computed separately for each considered time period and climate scenario using interpolated climate surfaces from the WorldClim database (Hijmans *et al* 2005). The database includes monthly air temperature averages and precipitation sums for the baseline period 1950–2000 (note that the majority of the permafrost landform observations were from this period) and for two future periods (2041–2060 and 2061–2080), for which we used RCP4.5 and RCP8.5 radiative forcing scenarios (van Vuuren *et al* 2011). Future climate projections included in the WorldClim database (Hijmans *et al* 2005) derive from an ensemble of 18 global climate models in the Coupled Model Intercomparison Project phase 5 archive (Taylor *et al* 2012).

The GMTED2010 digital elevation model (Danielson and Gesch 2011) at 30 arc-second spatial resolution (~1 km) was employed to compute the topography predictors, which were used to represent the amount of incoming solar energy, and the transport of ground material and moisture across the landscape. Potential incident solar radiation (McCune and Keon 2002) (PISR, MJ cm⁻² a⁻¹) was computed using slope, aspect and latitude, of which slope angle (Slope, °) was used also as an independent predictor in the modelling. PISR was omitted from pingo and ice-wedge polygon modelling, because in flat areas it is argued to reflect the latitudinal gradient rather than local topography-mediated insolation conditions (Karjalainen *et al* 2019). Topographic wetness index (TWI) was computed in SAGA GIS (System for Automated Geoscientific Analyses, Conrad *et al* 2015) with the SAGA Wetness Index tool (Böhner and Selige 2006), all the other predictors in ArcGIS 10.5.

Averaged proportions of coarse sediments (Coarse, grain size > 2 mm) and fine sediments (Fine, [sum of clay and silt] < 50 μm) as well as the content of soil organic carbon (SOC, g kg⁻¹) within 2 m from the surface were derived from the Soil-Grids database (Hengl *et al* 2017). These factors were assumed to characterize the varying hydro-thermal conditions of permafrost soils. Finally, we determined water coverage (%) in the 30 arc-second grid cells using a 150 m resolution dataset on water bodies (Defourny 2016) to account for the proportion of thawed ground (lakes and taliks) in each grid cell. There also exist site-specific factors that we could not directly consider with geospatial data at a circum-polar extent. Pingo and ice-wedge polygon formation depends on groundwater flow, and the thickness and water flow permeability soil deposits (Jones *et al* 2012), while debris availability, lithology and melt-water dynamics are central for rock glaciers (Lilleøren and Etzelmüller 2011, Knight *et al* 2019).

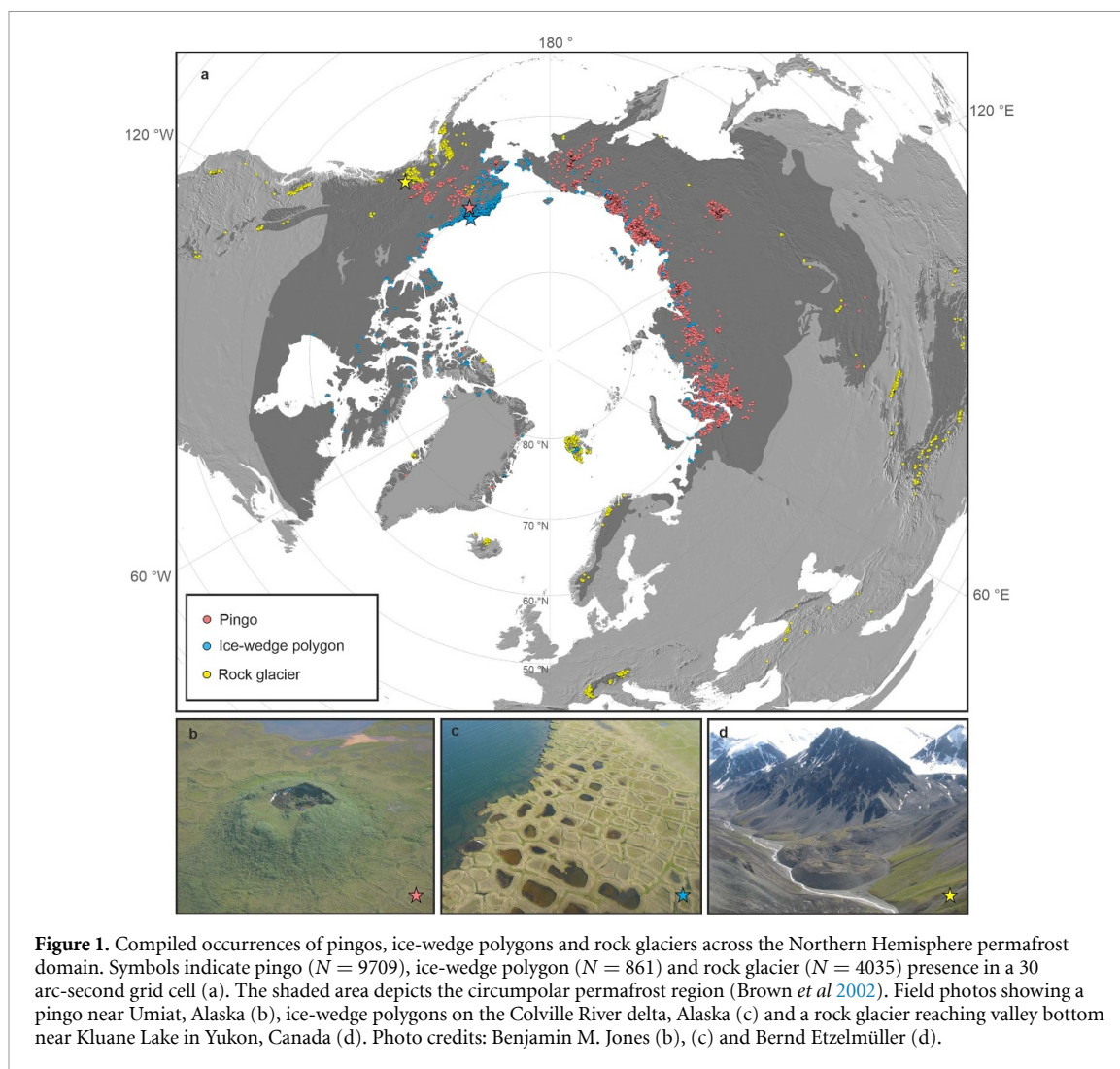


Figure 1. Compiled occurrences of pingos, ice-wedge polygons and rock glaciers across the Northern Hemisphere permafrost domain. Symbols indicate pingo ($N = 9709$), ice-wedge polygon ($N = 861$) and rock glacier ($N = 4035$) presence in a 30 arc-second grid cell (a). The shaded area depicts the circumpolar permafrost region (Brown *et al* 2002). Field photos showing a pingo near Umiat, Alaska (b), ice-wedge polygons on the Colville River delta, Alaska (c) and a rock glacier reaching valley bottom near Kluane Lake in Yukon, Canada (d). Photo credits: Benjamin M. Jones (b), (c) and Bernd Etzelmüller (d).

2.3. Statistical modelling

We modelled the suitable environmental spaces for landform occurrence and factors affecting their distribution by relating the compiled observations of landform presence and absence to environmental conditions using multivariate statistical methods. We used four methods and model-averaging techniques (Aalto *et al* 2017) to reduce the prediction uncertainty related to the choice of a single modelling method (Thuiller *et al* 2009). Generalized linear modelling (GLM), generalized additive modelling (GAM), generalized boosting modelling (GBM) and random forest (RF), were implemented within BIOMOD2 environment (Thuiller *et al* 2009) in R (version 3.5.2, see model calibration details in section 2, supplementary material). Model evaluation was performed using 100-fold cross validation that at each run used a random sample of 70% of observations in the datasets to calibrate a model and to validate it with the remaining 30%. Model performance was evaluated at each round with the adjusted coefficient of determination (R^2) and two prevalence-independent statistical measures of classification accuracy; area under

the receiving operating characteristic curve (AUC) and true skill statistic (TSS, Allouche *et al* 2006). Ensemble predictions were then formed by using the committee-averaging algorithm (Thuiller *et al* 2009, section 2, supplementary material). We evaluated the spatial reliability of the predictions by mapping the modelling agreement between the four methods (Luoto *et al* 2010).

To examine the environmental controls and sensitivities of permafrost landforms we estimated a modelling technique-independent variable importance score for each predictor (Thuiller *et al* 2009), and created response curves with each of the four methods to examine the shapes of relationships between each landform and predictors (Elith *et al* 2005) using response.plot2 function in BIOMOD2 environment (Thuiller *et al* 2009).

Projections for 2041–2060 and 2061–2080 were performed by substituting the climate parameters in the calibrated models with respective climate change scenario-based predictors (Hijmans *et al* 2005). Other predictors were not modified (Aalto *et al* 2017, 2018) but used as they were in the baseline modelling

in order to constrain suitable topography, surficial deposits and drainage conditions for landform occurrence in changing climatic conditions. These factors were considered to remain relatively unchanged within the study period, while vegetation properties that affect permafrost-climate responses (Shur and Jorgenson 2007) were assumed to change unpredictably, and thus not accounted for. Finally, areal coverages of projected environmental spaces were clipped and computed inside a recent permafrost zonation (Obu *et al* 2019). This delineation considers isolated permafrost areas in higher detail than the International Permafrost Association map (Brown *et al* 2002).

3. Results

Based on the predicted environmental spaces for current and future time periods, we classify three pathways of suitability for landform occurrence; 1) persisting conditions with suitable topographic and soil conditions for landform occurrence and climate remaining favourable, 2) environmental space loss, in which climatic conditions become unsuitable, and 3) new environmental spaces with potential for occurrences outside current distribution (i.e. suitable topography, soil and newly formed climatic conditions). Finally, we examine the factors affecting landform occurrence and evaluate the reliability of the predictions.

3.1. Regional changes in environmental spaces

Based on ensemble modelling, the predicted current coverage of environmentally suitable spaces is 2.04×10^6 km² for pingos, 3.12×10^6 km² for ice-wedge polygons and 1.40×10^6 km² for rock glaciers (figure 2, union of orange and red zones). Under the moderate 2041–2060 climate-forcing scenario (RCP4.5), the total areas of potential environmental spaces for the studied permafrost landforms are predicted to reduce to 1.44×10^6 km² (by 29%), 2.47×10^6 km² (21%) and 1.08×10^6 km² (23%), respectively (figure 2, supplementary tables 2 and 3). By 2061–2080, assuming the RCP8.5 scenario, on average over 50% of recent environmental spaces may be lost.

The largest losses of environmental spaces for pingos and ice-wedge polygons are concentrated on northwestern Russia and the middle reaches of major Arctic rivers (figures 2(a) and (b)). In the zone of discontinuous permafrost, suitable conditions for rock glacier occurrence show a distinctive shift towards higher elevations. As a result, areal losses are projected in most areas of current occurrences (figure 2(c)). In continuous permafrost regions, the projected losses are generally small.

New environmental spaces are projected to emerge where air temperatures and precipitation attain suitable levels for occurrence and other factors

are favourable. For pingos and ice-wedge polygons, new suitable areas (circumpolar totals of 0.67 and 0.33×10^6 km²) predominantly situate across Canada's Arctic Archipelago and in the Taymyr Peninsula (figures 2(a) and (b)). Pingo environments show a poleward shift, while suitable conditions for ice-wedge polygons are predicted in diverse landscapes amidst the recent occurrences. However, suitability for recent pingos, also, is predicted in many locations on Canada's Arctic islands even though not visible in the small-scale map (figure 2(a)). The largest areal increases in potentially suitable conditions for rock glacier occurrence (0.15×10^6 km²) appear in northern Alaska, high-Arctic Canada, eastern Greenland and Far-Eastern Russia (figure 2(c)). The general trajectory of the changes is towards colder regions of continuous permafrost. Based on the climate-change scenarios, both air temperature and rainfall show distinct increases at grid cells with observed landform occurrences (figure 3). Snowfall is projected to decrease at rock glacier sites, in contrast to the increase in rainfall (figures 3(c) and (d)).

3.2. Climatic controls and sensitivity of permafrost landforms

According to the analyses of variable importance and response shapes, the optimal conditions for pingos and ice-wedge polygons at a circumpolar scale are similar (figures 4(a)–(c), supplementary figure 3) and characterized by flat topography with moderately high soil moisture, low rain- and snowfall (<~300 mm), and TDD (°C-days) of less than ~2000. For ice-wedge polygons, FDD also have a notable contribution indicating that their occurrence requires at least ~2500 °C-days. Notably, figure 3 suggests that FDD will drop below 2000 at many pingo and ice-wedge polygon sites regardless of the climate-change scenario.

Rock glacier occurrence increased on coarse-sediment slopes with low wetness index, TDD less than ~1200 °C-days, and FDD between ~1000 and 4500 °C-days (figure 4(d)). Increased probability of occurrence towards minimum FDD values in the dataset suggests that rock glaciers exist across a wide range of cold climates although most landforms in the dataset have relatively high FDD values (figure 3(b)). Each landform shows a clear decline in probability of occurrence when TDD exceeds ~1000 °C-days (figures 4(b)–(d)). The response of rock glaciers to increasing TDD is especially sharp. An even more abrupt threshold is found between rainfall and both pingos and ice-wedge polygons.

3.3. Statistical and spatial evaluations

To assess model fit and predictive performance we used a split-sample approach; the models were calibrated using 70% of the data and evaluated against the remaining 30% of observations. Based on 100-fold

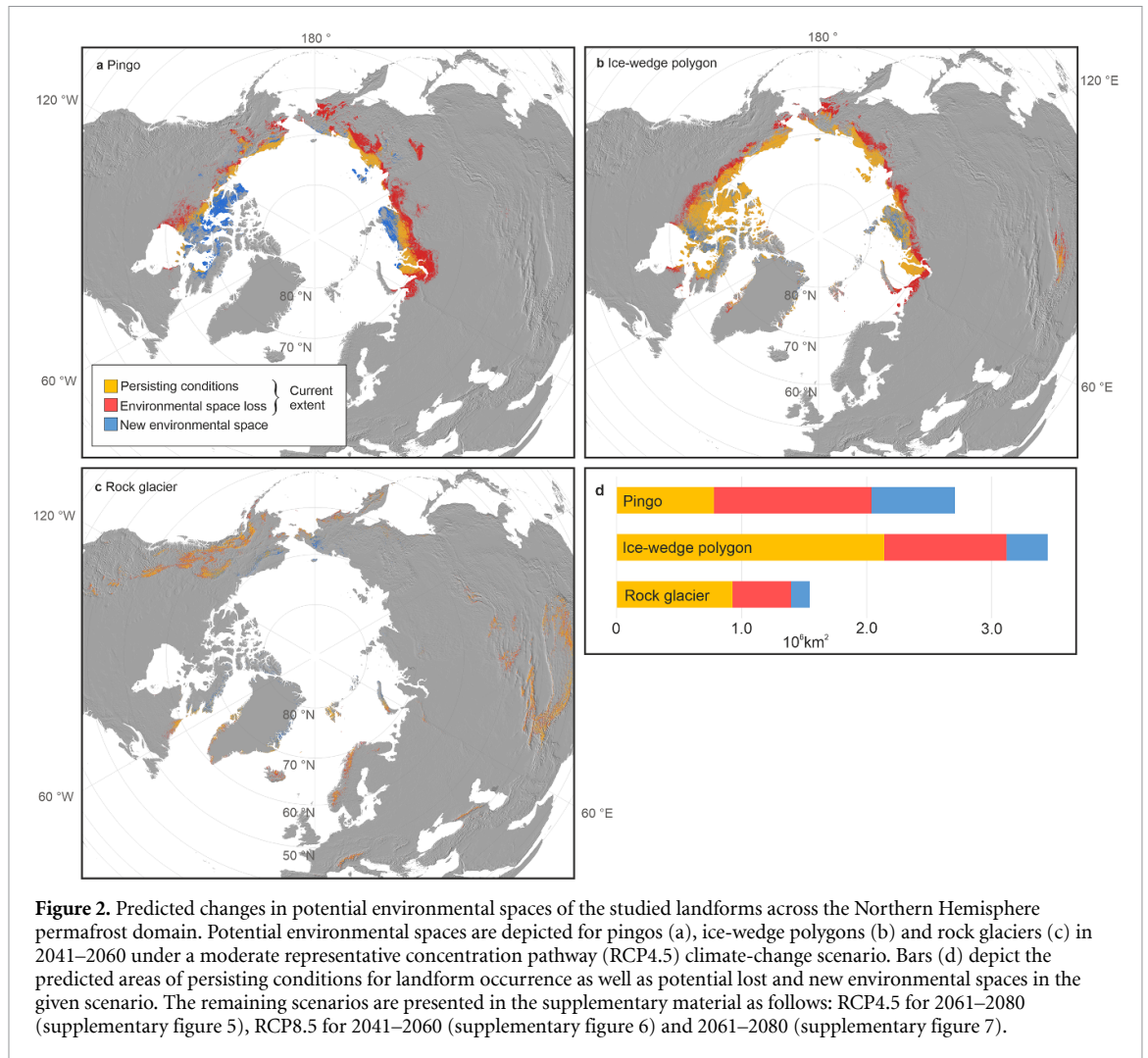


Figure 2. Predicted changes in potential environmental spaces of the studied landforms across the Northern Hemisphere permafrost domain. Potential environmental spaces are depicted for pingos (a), ice-wedge polygons (b) and rock glaciers (c) in 2041–2060 under a moderate representative concentration pathway (RCP4.5) climate-change scenario. Bars (d) depict the predicted areas of persisting conditions for landform occurrence as well as potential lost and new environmental spaces in the given scenario. The remaining scenarios are presented in the supplementary material as follows: RCP4.5 for 2061–2080 (supplementary figure 5), RCP8.5 for 2041–2060 (supplementary figure 6) and 2061–2080 (supplementary figure 7).

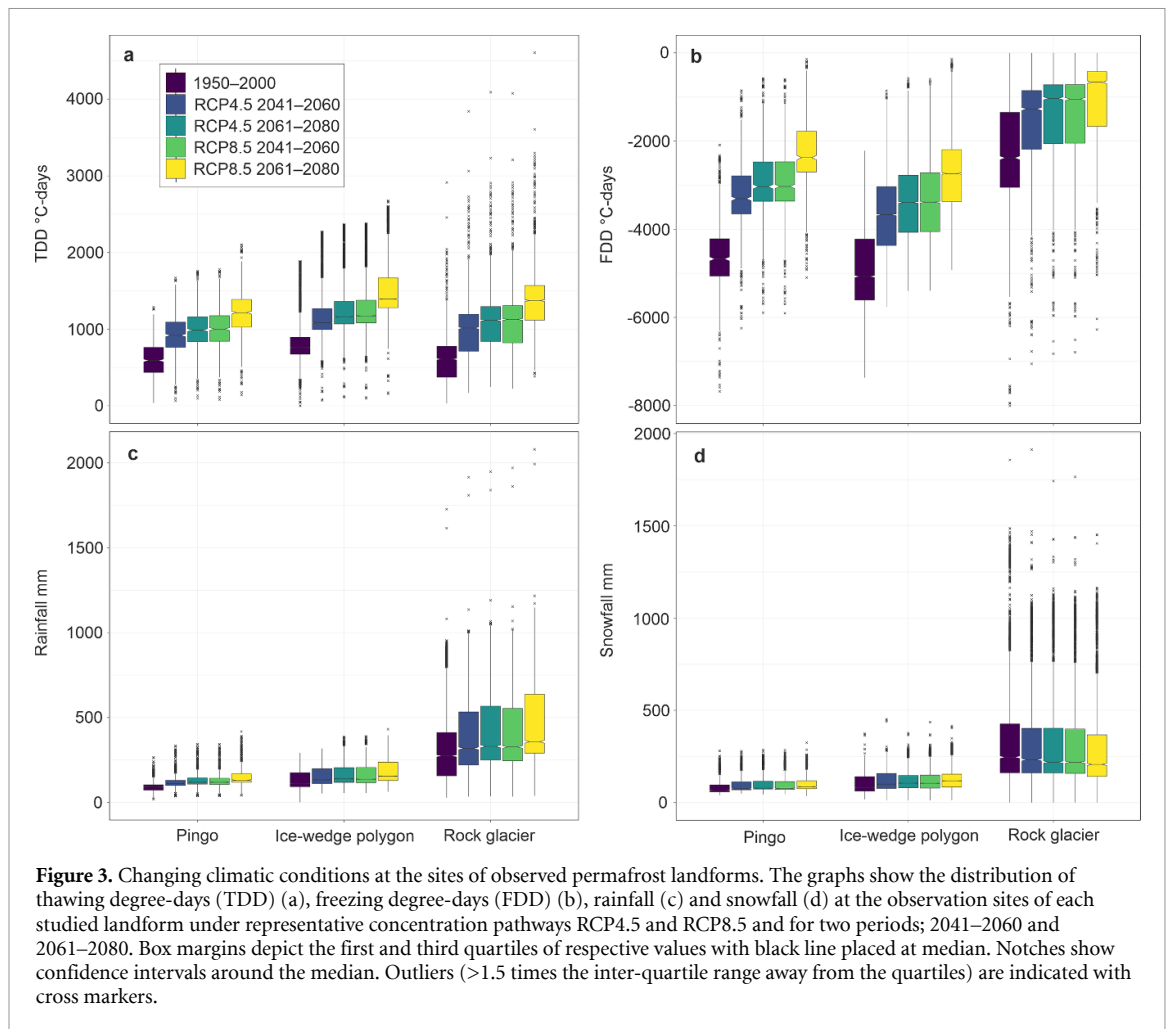
cross-validation, our approach predicted well the permafrost landform occurrences (figure 5). Ensemble method yielded the highest classification accuracy (AUC and TSS) in all cases and thus superior performance. Rock glacier models had the highest R^2 , AUC and TSS values, yet respective ensemble averages in pingo and ice-wedge polygon models also indicated excellent predictive performance. Moderate between-model variability was observed. GBM and RF best explained the variation in each landform occurrence having R^2 values at or above 0.90 (figure 5).

In key regions of landform distribution, the models largely agreed (figure 6). High inter-model variability was encountered in poorly sampled regions, such as the Tibetan Plateau where GLM and GAM predicted notably larger ice-wedge polygon distributions than GBM and RF, which both yielded more constrained environmental spaces (figure 6(d)). The lower evaluation statistics of GLM and GAM in pingo modelling (figure 5(a)) may explain the model disagreement in many regions (figure 6(a)). In cases like these, the ensemble method facilitates controlling for prediction uncertainty by

allowing for a conservative model agreement-based assessment. Despite superior model performance, ensemble models failed to identify a few known regions for observed occurrence. For example, only GBM and RF predicted pingo occurrence potential in Svalbard and eastern Greenland (figure 6(a)). Evaluations of spatial uncertainty such as presented here help identifying regions and environmental conditions where additional investigations should be made and thereby improve future model performance.

4. Discussion

The predicted losses of environmental spaces are largely associated with regions of projected near-surface permafrost thaw in the near future due to warming climate (e.g. Slater and Lawrence 2013, Chadburn *et al* 2017), but not exclusively, as areas of continuous permafrost in, e.g. northern Siberia may also become unsuitable for pingos and ice-wedge polygons. Based on our analyses, the environmental suitability for these landforms will be foremostly constrained by increasing TDD and rainfall. These



findings suggest that warmer and wetter summers, and the projected thickening of the active layer (Aalto *et al* 2018, Peng *et al* 2018) can melt pingo ice (Grosse and Jones 2011) and ice wedges close to the ground surface in these regions, as observed elsewhere in the Arctic (e.g. Fortier *et al* 2007, Liljedahl *et al* 2016, Bernard-Grand'Maison and Polard 2018, Farquharson *et al* 2019). First studies considering thermokarst-inducing processes in a numerical model indeed project substantial surface permafrost degradation and widespread landscape collapse even for the currently still cold North-East Siberian permafrost region under a strongly warming climate scenario (RCP8.5) (Nitzbon *et al* 2020), which is largely in line with our findings. Alongside increasing air temperatures, increased rainfall has been shown to stimulate permafrost thaw (Douglas *et al* 2020).

Importantly, predicted losses do not imply complete thaw of permafrost at depth but rather that the permafrost landforms can be lost due to conditions becoming unfavourable for their occurrence. However, ground ice in the landforms can be still protected from thaw by ecosystem properties, such as insulation by thick layers of peat (Shur and Jorgenson 2007) or cooling effect of cold air circulation in blocky rock glacier surfaces (Jones *et al* 2019).

Local hydro-topographical and ecological properties can also determine whether prolonged degradation leads to drainage or wetting of landscape, and thus the potential release of greenhouse gases (Jorgenson *et al* 2015, Liljedahl *et al* 2016, Nitzbon *et al* 2020).

Rainfall was the most important single variable delineating suitable conditions for pingos and ice-wedge polygons at the circumpolar scale, while TWI and FDD foremostly affected rock glacier occurrence potential. Even though these were central factors, the results implied that local topography and soil properties hold notable roles in constraining finer scale environmental suitability for the landforms. Based on the findings, it is suggested that increases in the amount of rainfall to above ~ 200 mm (figures 4(b) and (c)) can severely limit pingo and ice-wedge polygon occurrence potential. In the case of ice-wedge polygons, TDD had nearly as an important of a contribution suggesting that air temperature is the central factor for their occurrence. Pingos also showed a secondary relation to TDD yet rainfall was more dominant in their case.

The effect of rainfall is due arguably to the increased conduction of heat into the ground (Jorgenson *et al* 2006, Iijima *et al* 2010) but also the

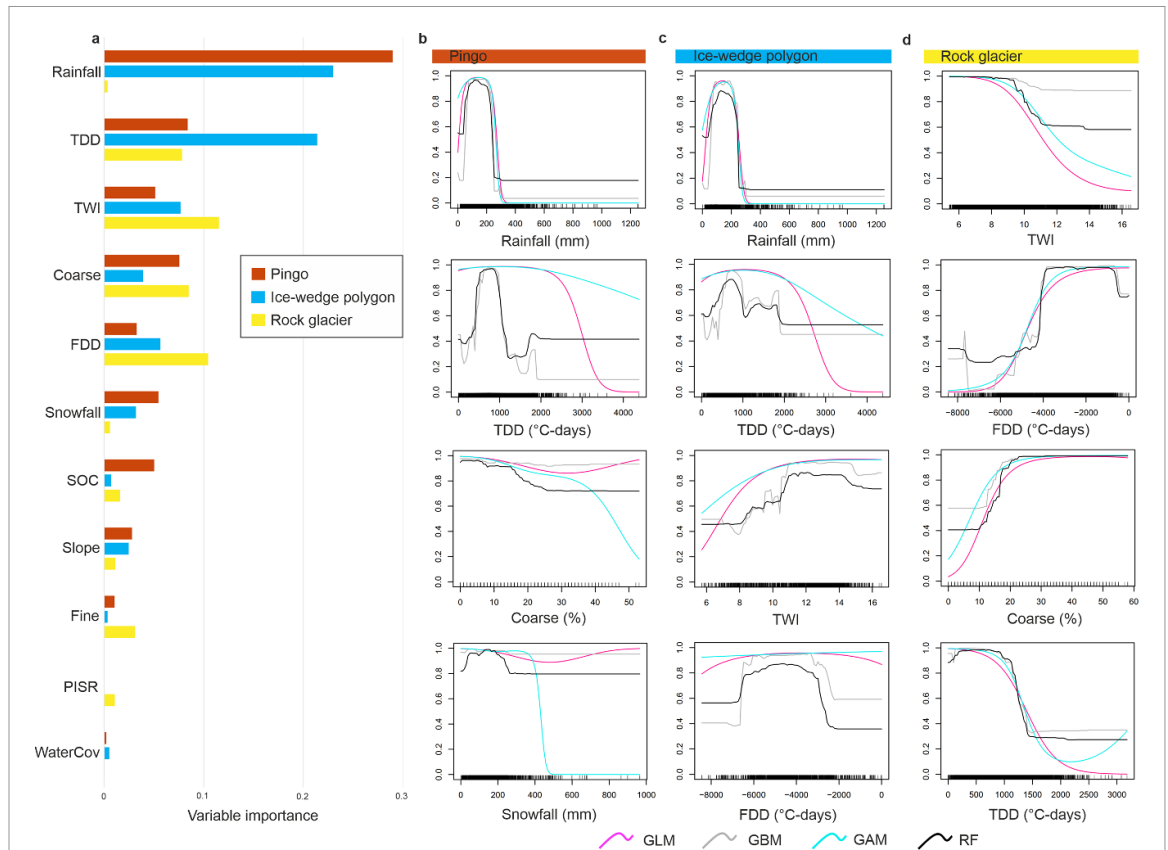


Figure 4. The relative importance of environmental factors for the studied landforms and response curves for the key predictors. Variable importance scores for individual environmental predictors based on average over four models (results from generalized linear model (GLM), generalized boosting method (GBM), generalized additive model (GAM), and random forest (RF)) are presented for pingos, ice-wedge polygons and rock glaciers (a). Response curves show the fitted response shapes of four most important predictors with pingos (b), ice-wedge polygons (c) and rock glaciers (d), i.e. when other predictors are held constant at their mean value (Elith *et al* 2005). The response curves for the remaining predictors are presented in supplementary Figure 3. Abbreviated predictors are thawing- and freezing degree-days (TDD and FDD, °C-days), topographic wetness index (TWI), soil organic carbon content (SOC, g kg⁻¹), coarse and fine sediment proportions (Coarse and Fine, %), slope angle (Slope, °), coverage of water bodies (WaterCov, %), and potential incident solar radiation (PISR, MJ cm⁻² a⁻¹).

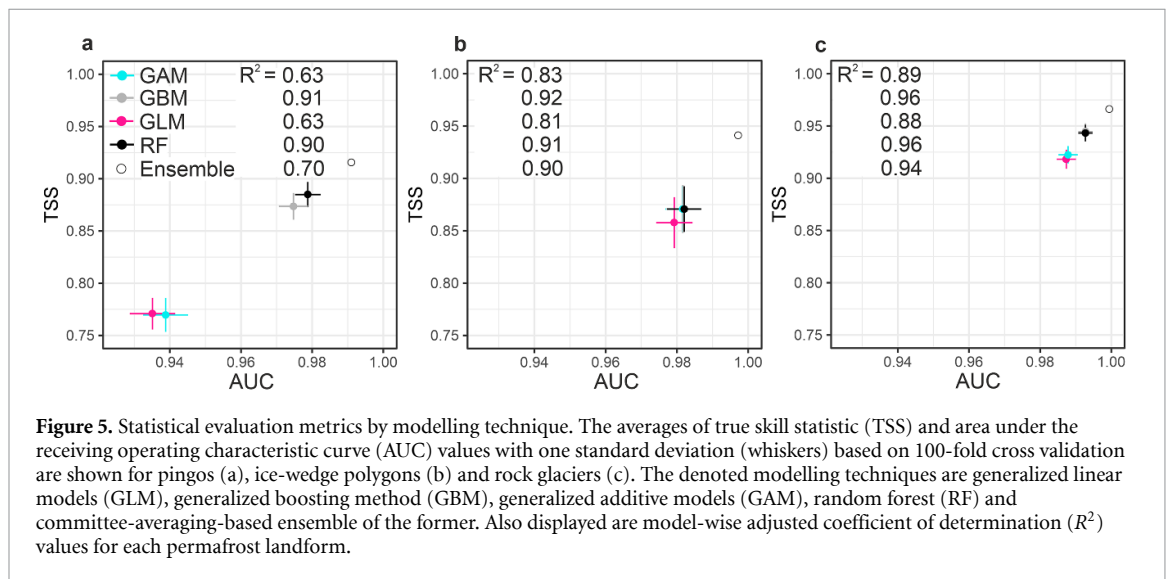
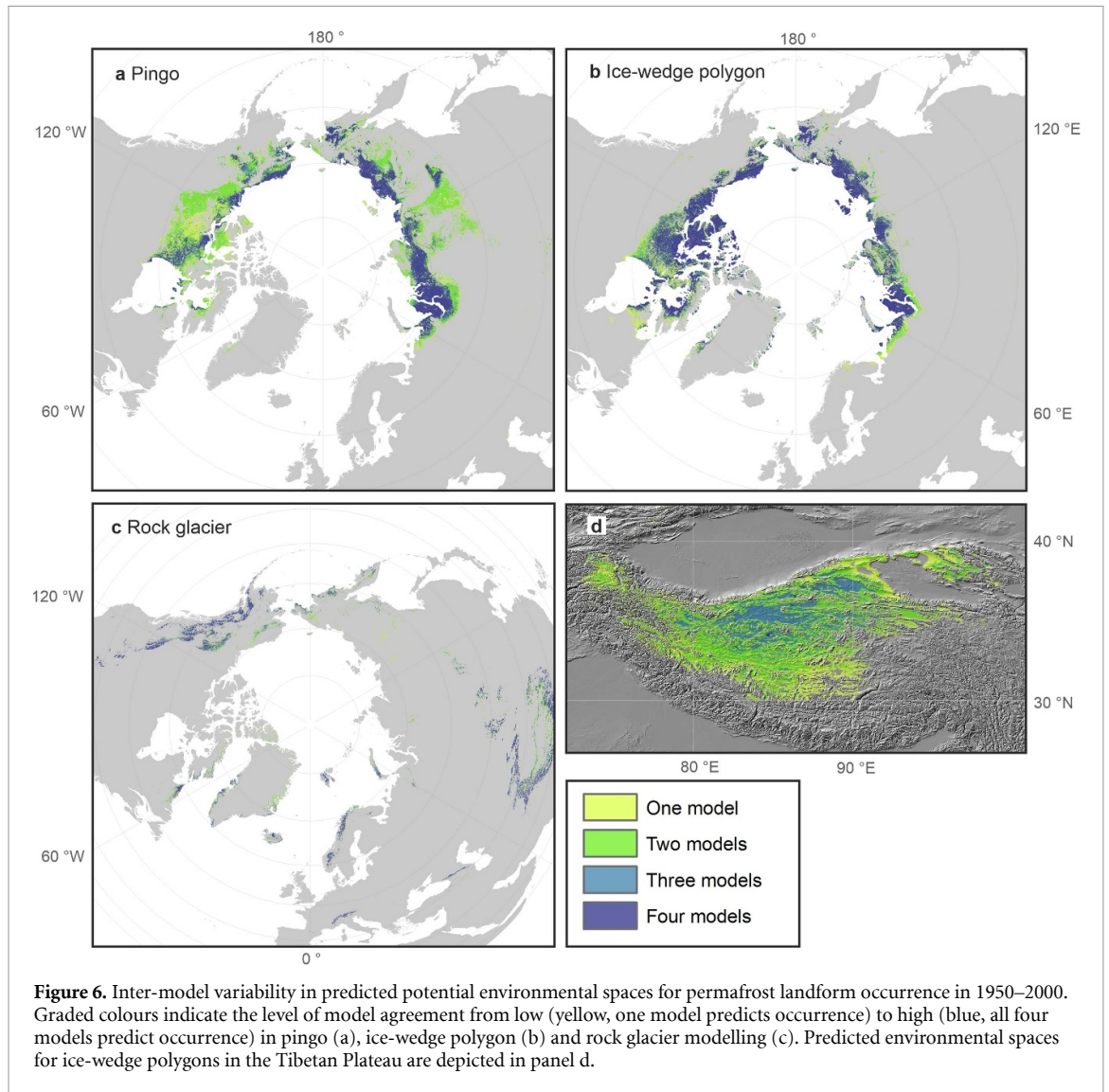


Figure 5. Statistical evaluation metrics by modelling technique. The averages of true skill statistic (TSS) and area under the receiving operating characteristic curve (AUC) values with one standard deviation (whiskers) based on 100-fold cross validation are shown for pingos (a), ice-wedge polygons (b) and rock glaciers (c). The denoted modelling techniques are generalized linear models (GLM), generalized boosting method (GBM), generalized additive models (GAM), random forest (RF) and committee-averaging-based ensemble of the former. Also displayed are model-wise adjusted coefficient of determination (R^2) values for each permafrost landform.

introduction of advective heat (Kane *et al* 2001). Rainfall also has been shown to induce abrupt thaw processes in ice-rich permafrost terrain (Kokelj *et al* 2015). Owing to the nonlinear response shape, the

found effect also applies the other way; suitable conditions can emerge if currently very dry areas begin to receive higher rainfall (>~100 mm, figures 4(b) and (c)) in the future, provided that air temperature and



other conditions are suitable. Some of rainfall's contribution could be attributed to its moderately strong correlation with TDD in the modelling data (supplementary figure 4). Notwithstanding, the analysis of variable importance suggested that rainfall had a greater relative effect than TDD, especially for pingos (figure 4(a)).

The responses of pingos and ice-wedge polygons with rainfall, and rock glaciers with air temperature, were strong and supported by each method. The projections of future climate, however, include uncertainty, especially in mountainous areas (Hijmans *et al* 2005, Hoegh-Guldberg *et al* 2018). The interpolated climate surfaces cannot fully account for orographic precipitation patterns or wind-induced snow transport, for example. Ice-wedge polygons' response to snowfall indicated a lowered occurrence probability with increasing snowfall (supplementary figure 3) in line with the observations by Kokelj *et al* (2014). However, climatic predictors averaged over a series of decades cannot represent future dynamics

of snow depth-controlled frost cracking under wintertime cold spells or other extreme air temperature, precipitation or disturbance (i.e. fire) events, which play a role in the formation and degradation of especially ice-wedge polygons (Jorgenson *et al* 2006, Jones *et al* 2015, Liljedahl *et al* 2016, Kanevskiy *et al* 2017). Based on experimental evidence (Allard and Kasper 1998, Christiansen 2005), thermal contraction cracking occurs during prolonged cooling periods with ground temperatures below -20 to -15 °C. In this study, the moderate importance of FDD and snowfall for ice-wedge polygons suggests that higher temporal resolution of climate predictors (monthly to sub-monthly) and a more explicit representation of snow cover variation are needed to estimate thermal cracking potential.

Recent studies show that ice-wedge polygons formed in centennial to millennial time scales can be lost by melting of their uppermost portion in a few decades (Jorgenson *et al* 2006, Liljedahl *et al* 2016, Fraser *et al* 2018, Farquharson *et al* 2019).

Large pingos with thick insulating overburdens are to a degree resilient to short-term changes in climate (Mackay 1998), but evidence of collapsed and paleo-pingos in concurrent non-permafrost environments confirms their climate sensitivity over longer time scales (Vandenberghe and Pissart 1993, Jones *et al* 2012). Degradation of ice-wedge polygons at local scales demonstrates large spatial variation owing to complex interactions between, e.g. ground ice, wetness conditions and microtopography (Kanevskiy *et al* 2017, Steedman *et al* 2017, Fraser *et al* 2018, Nitzbon *et al* 2019, 2020). Notwithstanding, some have argued that future thermokarst rates at broader scales mainly depend on the magnitude of regional climate change (Olefeldt *et al* 2016). Degradation of any of the studied permafrost landforms can also occur due to their natural lifecycles without external forcing (Washburn 1980, Mackay 1988).

Few quantitative or spatial estimates exist to compare with the predicted coverages. Mackay (1972) estimated that ice-wedge polygons covered 2.6×10^6 km² of the Northern Hemisphere, which falls relatively close to our ensemble prediction for 1950–2000 (3.1×10^6 km²). On a regional level, our ice-wedge polygon predictions for the main occurrence areas are in line with a recent Canada-wide modelling of wedge-ice content (O'Neill *et al* 2019), yet regional discrepancies are visible (section S3, supplementary material).

The discrepancies between the models (figures 4 and 5) are argued to have stemmed from different initial model assumptions and parameterizations (Thuiller *et al* 2009). For example, only GBM and RF captured a decline in rock glacier occurrence probability when FDD approached zero, i.e. milder freezing-season conditions (figure 4(d)). GLM and GAM overlooked this threshold and extended to too warm and flat areas, such as periglacial environments more characteristically affected by extensive solifluction processes, e.g. in northern Scandinavia (Aalto *et al* 2017). The wide distribution may also have been partly attributed to the inclusion of moraine-derived rock glaciers (section 1, supplementary material) which are easily mixed with debris-covered glaciers, and thus may extend below lower permafrost boundary limits. Moreover, some of the compiled observations might have been relict rock glaciers, and thus possibly lacked permafrost, as suggested by relatively high TDD and FDD for many objects in the dataset (figures 3(a) and (b)). The discrimination of intact rock glaciers from these landforms is often challenging, especially from optical remote sensing data from which a large part of observations was mapped.

Considering the projected new regions with suitable environmental spaces for landforms, we argue that the dependency of landform growth on local geomorphic and hydrologic conditions and glacial history means that they are likely to occur in more constrained environments than estimated in this study.

Prediction of pingo formation potential, for example, is difficult owing to its dependency on special groundwater pressure conditions (governed by underlying substrate properties) and dynamic processes such as lake drainage (Mackay 1998). Here, coarse sediments showed moderate importance and realistic response shapes with the landforms. Due to relatively few observations of soil properties within the permafrost domain available to produce the soil data layers (Hengl *et al* 2017), the data used here likely have a limited ability in depicting landform-scale variation in grain size proportions. Moreover, although we argue that the ~1 km resolution is sufficient to delineate topo-climatic conditions for most rock glaciers, there remains a need to account for site-specific debris availability, lithology and melt-water dynamics, or groundwater conditions and sedimentary history in the cases of pingos and ice-wedge polygons. Not considering all constraining factors for landform development may cause modelling to overestimate the extent of new suitable conditions, and subsequently the presented proportions of lost environmental spaces are arguably conservative.

Ultimately, we model suitable conditions for landform occurrences in recent and future climates, but cannot presently address the physical processes, such as ground-ice degradation or aggradation and associated heat fluxes, behind landform development using our approach. The vulnerability of permafrost to atmospheric warming is highly complex and depends on multiple dynamic processes acting in the surface water, snow, vegetation and soil layers and related positive and negative feedbacks (Shur and Jorgenson 2007, Nitzbon *et al* 2019). Moreover, the thermal inertia of ice-rich ground encumbers permafrost warming (Grosse *et al* 2011). Ground ice and associated phase changes of water (i.e. the latent heat effect), as well as the content of unfrozen water in frozen soils (Hu *et al* 2020), are key constituents of the near-surface permafrost response to climate forcing that may not be uniform in different initial ground temperature conditions (Riseborough 1990). Not considering such transient effects lowers our ability to assess landform occurrence potential in the future, given that the used approach assumes equilibrium state between landforms and climate. Process-based models could be appropriate for assessing the physical responses and related feedbacks of climate change because of their explicit parameterization of heat fluxes and transient effects in the surface layers (e.g. Harris *et al* 2009). However, they are often conducted at coarse spatial resolutions, which limits their applicability in assessing permafrost landforms at a relevant scale in a hemispheric extent.

Statistical modelling allows for producing reasonably accurate information on the suitable environments for permafrost landforms at a high resolution. This information can be used to link locally resolved detailed land surface processes to globally

relevant developments due to climate change. Predictions can also facilitate initial landform mapping in understudied regions although their accuracy at pixel resolution ($\sim 1 \text{ km}^2$) is to be taken cautiously due to the documented prediction errors (figure 5). In addition to likely profound geomorphic changes, ground ice degradation in the areas of projected lost environmental conditions may greatly alter hydrological and biogeochemical processes. In addition, the eventual disappearance of permafrost landforms represents a loss in local geodiversity, and thereby affects biodiversity (Antonelli *et al* 2018). From a human activity point of view, ground ice degradation and loss of permafrost landforms can affect freshwater availability (Jones *et al* 2018, 2019) and infrastructure integrity (Raynolds *et al* 2014, Kanevskiy *et al* 2017). Using permafrost landforms as proxies for massive ice, our modelling yielded novel information on fine-scale spatial variation of high ground ice content across permafrost landscapes. It should be noted that pingos occupy a very small proportion of landscapes relative to ice-wedge polygonal terrain or even large rock glaciers, and thus the potential amount of ground ice expected in a grid cell is different for each landform.

5. Conclusions

From this study the following conclusions could be drawn:

- The suitable environmental conditions for permafrost landforms at the circumpolar scale are closely related to climate and prone to shift along projected regional changes in air temperature and precipitation.
- On average, the landforms are projected to lose more than one-fifth of their suitable environments under a moderate climate scenario (RCP4.5) and around one-third under a very high baseline emission scenario (RCP8.5) by midcentury.
- The sensitivity of pingos and ice-wedge polygons to the amount of rainfall was unambiguous, albeit TDD was almost as important for ice-wedge polygons.
- Alongside air temperatures, precipitation regime is suggested to be a key constraining factor of geomorphic development outside mountainous environments.
- For rock glaciers, air temperature and topography primarily controlled the occurrence potential. However, the approach had a limited ability to separate suitable environments for rock glaciers from those for other glacial or periglacial slope processes.

The predicted changes in environmental spaces suitable for the studied permafrost landforms will affect Arctic landscapes and their geomorphology across large areas. The potential implications should

be considered when assessing impacts of climate change on natural and human systems.

Acknowledgments

This study was funded by the Academy of Finland (grants 315519, 307761). BMJ was supported by awards from the US National Science Foundation (OPP-1806213 and ICER-1927872) and GG was supported by ERC PETA-CARB (#338335), the HGF Impulse and Networking Fund (ERC-0013), and NASA NNX08AJ37G. The contribution by BE and KSL was funded by the University of Oslo, Norway. We wish to thank two anonymous reviewers for their highly valuable comments.

Data availability statement

The data that support the findings of this study are available upon reasonable request from the authors.

Author contributions

OK, ML and JH developed the original idea. OK led the compilation of observational data with contributions from BE, GG, BMJ and KSL, and geospatial data processing with JH and JA. OK performed the statistical analyses with contributions from JA, JH and ML. OK wrote the manuscript with contributions from all the authors.

Competing interests

The authors declare that they have no competing interests.

ORCID iDs

Olli Karjalainen  <https://orcid.org/0000-0003-2429-4595>

Miska Luoto  <https://orcid.org/0000-0001-6203-5143>

Juha Aalto  <https://orcid.org/0000-0001-6819-4911>

Bernd Etzelmüller  <https://orcid.org/0000-0001-5156-3653>

Guido Grosse  <https://orcid.org/0000-0001-5895-2141>

Benjamin M Jones  <https://orcid.org/0000-0002-1517-4711>

Karianne S Lilleøren  <https://orcid.org/0000-0002-5887-1103>

Jan Hjort  <https://orcid.org/0000-0002-4521-2088>

References

- Aalto J and Luoto M 2014 Integrating climate and local factors for geomorphological distribution models *Earth Surf. Process. Landf.* **39** 1729–40

- Aalto J, Harrison S and Luoto M 2017 Statistical modelling predicts almost complete loss of major periglacial processes in Northern Europe *Nat. Commun.* **8** 515
- Aalto J, Karjalainen O, Hjort J and Luoto M 2018 Statistical forecasting of current and future circum-Arctic ground temperatures and active layer thickness *Geophys. Res. Lett.* **45** 4889–98
- Allard M and Kasper J N 1998 Temperature conditions for ice-wedge cracking: field measurements from Salluit, Northern Quebec *Proc. Seventh Int. Conf. on Permafrost* eds Allard M and Lewkowicz AG Centre d'études Nordiques, Université Laval pp 5–12
- Allouche O, Tsoar A and Kadmon R 2006 Assessing the accuracy of species distribution models: prevalence, kappa and the true skill statistic (TSS) *J. Appl. Ecol.* **43** 1223–32
- Antonelli A et al 2018 Geological and climatic influences on mountain biodiversity *Nat. Geosci.* **11** 718–25
- Barsch D 1996 *Rock-glaciers Indicators for the Present and Former Geocology in High Mountain Environments* (Berlin: Springer)
- Bernard-Grand'Maison C and Pollard W 2018 An estimate of ice wedge volume for a high arctic polar desert environment, Fosheim Peninsula, Ellesmere Island *Cryosphere* **12** 3589–604
- Berthling I 2011 Beyond confusion: rock glaciers as cryo-conditioned landforms *Geomorphology* **131** 98–106
- Biskaborn B K et al 2019 Permafrost is warming at a global scale *Nat. Commun.* **10** 264
- Boeckli L, Brenning A, Gruber S and Noetzi J A 2012 Statistical approach to modelling permafrost distribution in the European Alps or similar mountain ranges *Cryosphere* **6** 125–40
- Brighenti S, Tolotti M, Bruno M C, Wharton G, Pusch M T and Bertoldi W 2019 Ecosystem shifts in Alpine streams under glacier retreat and rock glacier thaw: a review *Sci. Total Environ.* **675** 542–59
- Brown J, Ferriars O J Jr, Heginbottom J A and Melnikov E S 2002 Circum-Arctic map of permafrost and ground-ice conditions version 2 (National Snow and Ice Data Center) <https://nsidc.org/data/ggd318>
- Böhner J and Selige T 2006 Spatial prediction of soil attributes using terrain analysis and climate regionalisation SAGA – *Analysis and Modelling Applications* eds Böhner J, McCloy KR and Strobl, J (Göttingen: Verlag Erich Goltze GmbH)
- Chadburn S E, Burke E J, Cox P M, Friedlingstein P, Hugelius G and Westermann S 2017 An observation-based constraint on permafrost loss as a function of global warming *Nat. Clim. Change* **7** 340–4
- Christiansen H H 2005 Thermal regime of ice-wedge cracking in Adventdalen, Svalbard *Permafrost Periglacial Process.* **16** 87–98
- Conrad O, Bechtel B, Bock M, Dietrich H, Fischer E, Gerlitz L, Wehberg J, Wichmann V and Böhner J 2015 System for automated geoscientific analyses (SAGA) v. 2.1.4 *Geosci. Model Dev.* **8** 1991–2007
- Danielson J J and Gesch D B 2011 Global multi-resolution terrain elevation data 2010 (GMTED2010 US geological survey open-file report 2011–1073) pp 26
- Defourny P 2016 *European Space Agency Land Cover Climate Change Initiative Water Bodies Map, v4.0 ESACCI-LC-L4-WB-Map-150m-P13Y-2000-v40* (Centre for Environmental Data Analysis) <http://maps.elie.ucl.ac.be/CCI/viewer/download.php>
- Douglas T A, Turetsky M R and Koven C D 2020 Increased rainfall stimulates permafrost thaw across a variety of Interior Alaskan boreal ecosystems *Npj Clim. Atmos. Sci.* **3** 28
- Elith J, Ferrier S, Huettmann F and Leathwick J 2005 The evaluation strip: A new and robust method for plotting predicted responses from species distribution models *Ecol. Modell.* **186** 280–9
- Evans D J A 1993 High-latitude rock glaciers: A case study of forms and processes in the Canadian arctic *Permafrost Periglacial Process.* **4** 17–35
- Farquharson L M, Romanovsky V E, Cable W L, Walker D A, Kokelj S and Nicolsky D 2019 Climate change drives widespread and rapid thermokarst development in very cold permafrost in the Canadian high arctic *Geophys. Res. Lett.* **46** 681–9
- Fewster R E, Morris P J, Swindles G T, Gregoire L J, Ivanovic R F, Valdes P J and Mullan D 2020 Drivers of Holocene palsa distribution in North America *Quat. Sci. Rev.* **240** 106337
- Fortier D, Allard M and Shur Y 2007 Observation of rapid drainage system development by thermal erosion of ice wedges on Bylot Island, Canadian Arctic archipelago *Permafrost Periglacial Process.* **18** 229–43
- Fountain A G, Campbell J L, Schuur E A G, Stammerjohn S E, Williams M W and Ducklow H W 2012 The disappearing cryosphere: impacts and ecosystem responses to rapid cryosphere loss *BioScience* **62** 405–15
- Fraser R H, Kokelj S V, Lantz T C, McFarlane-Winchester M, Olthof I and Lacelle D 2018 Climate sensitivity of high arctic permafrost terrain demonstrated by widespread ice-wedge thermokarst on banks Island *Remote Sens.* **10** 954
- Gorbunov A P 2013 Rock glaciers, glaciers and permafrost in Iran *Kriosfera Zemli* **17** 28–34
- Grosse G and Jones B M 2011 Spatial distribution of pingos in northern Asia *Cryosphere* **5** 13–33
- Grosse G, Romanovsky V, Jorgenson T, Walter Anthony K, Brown J and Overduin P P 2011 Vulnerability and feedbacks of permafrost to climate change *EOS* **92** 9
- Grosse G, Goetz S, McGuire A D, Romanovsky V E and Schuur E A G 2016 Changing permafrost in a warming world and feedbacks to the Earth system *Environ. Res. Lett.* **11** 040201
- Guo D and Wang H 2016 CMIP5 permafrost degradation projection: a comparison among different regions *J. Geophys. Res. Atmos.* **121** 4499–517
- Harris C et al 2009 Permafrost and climate in Europe: monitoring and modelling thermal, geomorphological and geotechnical responses *Earth Sci. Rev.* **92** 117–71
- Hengl T et al 2017 SoilGrids250m – global gridded soil information based on machine learning *PLoS ONE* **12** e0169748
- Hijmans R J, Cameron S E, Parra J L, Jones P G and Jarvis A 2005 Very high resolution interpolated climate surfaces for global land areas *Int. J. Clim.* **25** 1965–78
- Hjort J, Karjalainen O, Aalto J, Westermann S, Romanovsky V E, Nelson F E, Etzelmüller B and Luoto M 2018 Degrading permafrost put Arctic infrastructure at risk by midcentury *Nat. Commun.* **9** 5147
- Hoegh-Guldberg O et al 2018 Impacts of 1.5°C of global warming on natural and human systems *Global Warming of 1.5°C An IPCC Special Report on the impacts of global warming of 1.5°C above pre-industrial levels and related global greenhouse gas emission pathways, in the context of strengthening the global response to the threat of climate change, sustainable development, and efforts to eradicate poverty* eds Masson-Delmotte, V et al (Geneva: IPCC) pp 175–312
- Hu G, Zhao L, Zhu X, Wu X, Wu T, Li R, Xie C and Hao J 2020 Review of algorithms and parameterizations to determine unfrozen water content in frozen soil *Geoderma* **368** 114277
- Humlum O 2000 The geomorphic significance of rock glaciers: estimates of rock glacier debris volumes and headwall recession rates in West Greenland *Geomorphology* **35** 41–67
- Iijima Y, Fedorov A N, Park H, Suzuki K, Yabuki H, Maximov T C and Ohata T 2010 Abrupt increases in soil temperatures following increased precipitation in a permafrost region, central Lena River basin, Russia *Permafrost Periglacial Process.* **21** 30–41
- Jones B M, Grosse G, Hinkel K M, Arp C D, Walker S, Beck R A and Galloway J P 2012 Assessment of pingo distribution and morphometry using an IFSAR derived digital surface model, western Arctic coastal plain, Northern Alaska *Geomorphology* **138** 1–14
- Jones B M, Grosse G, Arp C D, Miller E, Liu L, Hayes D J and Larsen C F 2015 Recent Arctic tundra fire initiates widespread thermokarst development *Sci. Rep.* **5** p15865

- Jones D B, Harrison S, Anderson K and Betts R A 2018 Mountain rock glaciers contain globally significant water stores *Sci. Rep.* **8** 2834
- Jones D B, Harrison S, Anderson K and Whalley W B 2019 Rock glaciers and mountain hydrology: a review *Earth Sci. Rev.* **193** 66–90
- Jorgenson M T, Shur Y L and Pullman E R 2006 Abrupt increase in permafrost degradation in Arctic Alaska *Geophys. Res. Lett.* **33** L02503
- Jorgenson M T, Kanevskiy M, Shur Y, Moskalenko N, Brown D, Wickland K P, Striegl R G and Koch J C 2015 Role of ground ice dynamics and ecological feedbacks in recent ice wedge degradation and stabilization *J. Geophys. Res. Earth Surface* **120** 2280–97
- Kane D L, Hinkel K M, Goering D J, Hinzman L D and Outcalt S I 2001 Non-conductive heat transfer associated with frozen soils *Glob. Planet. Change* **29** 275–92
- Kanevskiy M, Shur Y, Jorgenson T, Brown D R N, Moskalenko N, Brown J, Walker D A, Reynolds M K and Buchhorn M 2017 Degradation and stabilization of ice wedges: implications for assessing risk of thermokarst in northern Alaska *Geomorphology* **297** 20–42
- Karjalainen O, Luoto M, Aalto J and Hjort J 2019 New insights into the environmental factors controlling the ground thermal regime across the Northern Hemisphere: a comparison between permafrost and non-permafrost areas *Cryosphere* **13** 693–707
- Knight J, Harrison S and Jones D B 2019 Rock glaciers and the geomorphological evolution of deglaciating mountains *Geomorphology* **324** 14–24
- Kokelj S V, Lantz T C, Wolfe S A, Kanigan J C, Morse P D, Coutts R, Molina-Giraldo N and Burn C R 2014 Distribution and activity of ice wedges across the forest-tundra transition, western Arctic Canada *J. Geophys. Res. Earth Surface* **119** 2032–47
- Kokelj S V, Tunnicliffe J, Lacelle D, Lantz T C, Chin K S and Fraser R 2015 Increased precipitation drives mega slump development and destabilization of ice-rich permafrost terrain, northwestern Canada *Glob. Planet. Change* **129** 56–68
- Kääb A, Frauenfelder R and Roer I 2007 On the response of rockglacier creep to surface temperature increase *Glob. Planet. Change* **56** 172–87
- Lara M J, Nitze I, Grosse G, Martin P and Mcguire A D 2018 Reduced arctic tundra productivity linked with landform and climate change interactions *Sci. Rep.* **8** 2345
- Liljedahl A K et al 2016 Pan-Arctic ice-wedge degradation in warming permafrost and its influence on tundra hydrology *Nat. Geosci.* **9** 312–8
- Lilleøren K S and Etzelmüller B 2011 A regional inventory of rock glaciers and ice-cored moraines in Norway *Geogr. Ann. Ser. A: Phys. Geogr.* **93** 175–91
- Luoto M, Marmion M and Hjort J 2010 Assessing spatial uncertainty in predictive geomorphological mapping: a multi-modelling approach *Comput. Geosci.* **36** 355–61
- Mackay J R 1972 The world of underground ice *Ann. Assoc. Am. Geogr.* **62** 1–22
- Mackay J R 1988 Pingo collapse and paleoclimatic reconstruction *Can. J. Earth Sci.* **25** 495–511
- Mackay J R 1998 Pingo Growth and collapse, Tuktoyaktuk Peninsula Area, Western Arctic Coast, Canada: a long-term field study *Géographie Phys. Quaternaire* **52** 271–323
- Mccune B and Keon D 2002 Equations for potential annual direct incident radiation and heat load *J. Vegetation Sci.* **13** 603–6
- Nitzbon J, Langer M, Westermann S, Martin L, Aas K S and Boike J 2019 Pathways of ice-wedge degradation in polygonal tundra under different hydrological conditions *Cryosphere* **13** 1089–123
- Nitzbon J, Westermann S, Langer M, Martin L C P, Strauss J, Labor S and Boike J 2020 Fast response of cold ice-rich permafrost in northeast Siberia to a warming climate *Nat. Commun.* **11** 2201
- O'Neill H B, Wolfe S A and Duchesne C 2019 New ground ice maps for Canada using a paleogeographic modelling approach *Cryosphere* **13** 753–73
- Obu J et al 2019 Northern Hemisphere permafrost map based on TTOP modelling of 2000–2016 at 1km² scale *Earth Sci. Rev.* **193** 299–316
- Olefeldt D et al 2016 Circumpolar distribution and carbon storage of thermokarst landscapes *Nat. Commun.* **7** 13043
- Peng X, Zhang T, Frauenfeld O W, Wang K, Luo D, Cao B, Su H, Jin H and Wu Q 2018 Spatiotemporal changes in active layer thickness under contemporary and projected climate in the northern hemisphere *J. Clim.* **31** 251–66
- Raynolds M K, Walker D A, Ambrosius K J, Brown J, Everett K R, Kanevskiy M, Kofinas G P, Romanovsky V E, Shur Y and Webber P J 2014 Cumulative geocological effects of 62 years of infrastructure and climate change in ice-rich permafrost landscapes, Prudhoe Bay Oilfield, Alaska *Glob. Change Biol.* **20** 1211–24
- Riseborough D W 1990 Soil latent heat as a filter of the climate signal in permafrost *Fifth Canadian Permafrost Conf.* (Québec: Université Laval) pp 199–205
- Rowland J C et al 2010 Arctic landscapes in transitions: responses to thawing permafrost *EOS* **91** 26
- Rudy A C A, Lamoureux S F, Treitz P, Ewijk K V, Bonnaventure P P and Budkewitsch P 2017 Terrain controls and landscape-scale susceptibility modelling of active-layer detachments, Sabine Peninsula, Melville Island, Nunavut *Permafrost Periglacial Process.* **28** 79–91
- Schuur E A G et al 2015 Climate change and the permafrost carbon feedback *Nature* **520** 171–9
- Serikova S et al 2018 High riverine CO₂ emissions at the permafrost boundary of Western Siberia *Nat. Geosci.* **11** 825–9
- Shur Y L and Jorgenson M T 2007 Patterns of permafrost formation and degradation in relation to climate and ecosystems *Permafrost Periglacial Process.* **18** 7–19
- Slater A G and Lawrence D M 2013 Diagnosing present and future permafrost from climate models *J. Clim.* **26** 5608–23
- Steedman A E, Lantz T C and Kokelj S V 2017 Spatio-temporal variation in high-centre polygons and ice-wedge melt ponds, Tuktoyaktuk coastlands, Northwest Territories *Permafrost Periglacial Process.* **28** 66–78
- Streletskiy D A, Suter L J, Shiklomanov N I, Porfiriev B N and Eliseev D O 2019 Assessment of climate change impacts on buildings, structures and infrastructure in the Russian regions on permafrost *Environ. Res. Lett.* **14** 025003
- Taylor K E, Stouffer R J and Meehl G A 2012 An overview of CMIP5 and the experiment design *Bull. Am. Meteorol. Soc.* **93** 485–98
- Thuiller W, Lafourcade B, Engler R and Araújo M B 2009 BIOMOD – a platform for ensemble forecasting of species distributions *Ecography* **32** 369–73
- van Vuuren D P et al 2011 The representative concentration pathways: an overview *Clim. Change* **109** 5–31
- Vandenbergh J and Pissart A 1993 Permafrost changes in Europe during the last glacial *Permafrost Periglacial Process.* **4** 121–35
- Ward Jones M K, Pollard W H and Jones B M 2019 Rapid initialization of retrogressive thaw slumps in the Canadian high Arctic and their response to climate and terrain factors *Environ. Res. Lett.* **14** 055006
- Washburn A L 1980 Permafrost features as evidence of climatic change *Earth Sci. Rev.* **15** 327–402